Physica A 390 (2011) 2855–2862

Contents lists available at ScienceDirect

Physica A

journal homepage: www.elsevier.com/locate/physa

Neural signal transduction aided by noise in multisynaptic excitatory and inhibitory pathways with saturation

Fabing Duan [a,*], François Chapeau-Blondeau [b], Derek Abbott [c]

[a] College of Automation Engineering, Qingdao University, Qingdao 266071, PR China

[b] Laboratoire d'Ingénierie des Systèmes Automatisés (LISA), Université d'Angers, 62 avenue Notre Dame du Lac, 49000 Angers, France

[c] Centre for Biomedical Engineering (CBME) and School of Electrical & Electronic Engineering, The University of Adelaide, Adelaide, SA 5005, Australia

ARTICLE INFO

Article history:
Received 22 November 2010
Received in revised form 23 January 2011
Available online 12 April 2011

Keywords:
Saturating dynamics
Inhibitory synapse
Correlation coefficient
Stochastic resonance

ABSTRACT

We study the stochastic resonance phenomenon in saturating dynamical models of neural signal transduction, at the synaptic stage, wherein the noise in multipathways enhances the processing of neuronal information integrated by excitatory and inhibitory synaptic currents. For an excitatory synaptic pathway, the additive intervention of an inhibitory pathway reduces the stochastic resonance effect. However, as the number of synaptic pathways increases, the signal transduction is greatly improved for parallel multipathways that feature both excitation and inhibition. The obtained results lead us to the realization that the collective property of inhibitory synapses assists neural signal transmission, and a parallel array of neurons can enhance their responses to multiple synaptic currents by adjusting the contributions of excitatory and inhibitory currents.

1. Introduction

The stochastic resonance phenomenon originally describes the match between the noise induced characteristic time scale of a system response and that of an input periodic subthreshold signal [1–4]. Gradually, different forms of stochastic resonance were shown to be feasible, with various types of signals, nonlinear systems, and measures of performance receiving improvement from noise [2–11]. For instance, suprathreshold stochastic resonance (SSR) occurring in an uncoupled parallel array breaks the restriction of a subthreshold input [7]. Subsequently, the input–output gain is enhanced by noise in array of static [11–16] or dynamical [17,18] nonlinear elements and has been demonstrated to exceed unity, which cannot be obtained by linear systems. Up to the present, the terminology *stochastic resonance* is used very frequently in the much wider sense of being the occurrence of any kind of noise-enhanced or noisy constructive phenomena in nonlinear systems [6]. Thus, stochastic resonance should be regarded as a complex phenomenon, and its key feature is the constructive role of noise. In this broad sense, many noise-enhanced phenomena such as the noise-induced linearization [19,20] and dithering [21,22] can be also contained within the conceptual framework of stochastic resonance [1–4,6].

Usually, the appearance of stochastic resonance is closely tied to nonlinear systems working in a noisy environment [1–3,6]. Therefore, due to nonlinearity within neurodynamics and the prevalently noisy environment of neural systems, the observations of stochastic resonance in such single neuron models as the FitzHugh–Nagumo model [3,23–27], integrate-fire model [28–32], threshold model [33,34,26,35], Hodgkin–Huxley model [36], neural network models [26,37–48] and real neurons [49–56] are progressively and continuously reported. So far, the main scenario of stochastic resonance occurring in

* Corresponding author.
E-mail addresses: fabing.duan@gmail.com, fabing1974@yahoo.com.cn (F. Duan).

0378-4371/$ – see front matter © 2011 Elsevier B.V. All rights reserved.
doi:10.1016/j.physa.2011.03.039

neural systems is the response of a neuron to a threshold or potential-barrier nonlinearity [2,3,23–25,28]. However, another form of stochastic resonance is recently reported exploiting a saturating nonlinearity [12,15,57], wherein no threshold or potential barrier is bestowed. In a recent paper [57], we demonstrated that essentially saturating dynamics, which is present in synaptic transduction, can give rise to stochastic resonance or an improvement via noise at this stage of neural signal transmission. Compared to threshold or potential-barrier dynamics, the improvement by noise via saturating dynamics takes place in more demanding conditions, wherein the inherent fluctuations of spontaneous firing rate or number of released neurotransmitter vesicles realize a non-negative noise representing these non-negative quantities at the synaptic stage [57]. This non-negative character of noise is attached to the neural interpretations of several stages of neural signal transmission [12,15,57,58].

In our previous study of stochastic resonance [57], we only considered a single synaptic pathway modeling the excitable synapse governed by saturating dynamics. However, realistic models of neurodynamics must ultimately encompass multiple interacting modules, and the neural information processing is the integration of excitatory and inhibitory synaptic contributions [59–68]. In the present paper, we first consider two synaptic pathways, i.e. one being excitatory and the other being inhibitory. The sum of both excitatory and inhibitory synaptic currents is then taken as the relevant output of these two synaptic pathways. Subsequently, the uncoupled parallel array of multiple synaptic pathways composed of a number of excitatory synapses and inhibitory synapses is considered. We numerically analyze the constructive role of noise from the inhibitory synaptic pathway for neuronal signal transduction, and also investigate the effect of the efficacy parameters of multisynaptic pathway on stochastic resonance or improvement of signal transmission by noise. The obtained results will lead to research attention on more elaborate dynamics for information improvement by noise in the nervous systems operated with saturating nonlinearity.

2. Model and measure

At the synaptic stage, neural signal transduction relies on neurotransmitter release and gating of ion channels. In the case of strong sustained presynaptic activity, both neurotransmitter pools and populations of ion channels can all be recruited in the process, therefore limiting any further increase of the electric current induced across the membrane of the postsynaptic neuron. This process can be described by the saturating dynamics [57–61]

$$\frac{\mathrm{d}I_j(t)}{\mathrm{d}t} = -\frac{I_j(t)}{\tau} + [I_{\mathrm{sat},j} - I_j(t)]w_j e_j(t), \tag{1}$$

where $I_j(t)$ denotes the synaptic current of an excitatory or inhibitory synapse j, τ represents the relaxation time of saturating dynamics, and the saturation current $I_{\mathrm{sat},j}$ is positive for an excitatory synapse j and negative for an inhibitory synapse j [60–63]. Here, the positive parameter w_j measures the efficacy of synapse j in converting the non-negative presynaptic activity $e_j(t)$ into a postsynaptic current $I_j(t)$ [58].

As we have interpreted the saturating dynamics of Eq. (1) in our previous study [57], the input signal $e_j(t)$ in Eq. (1) is non-negative, and represents the presynaptic activity at the input of the transmission pathway. Here, we assume that these synapses are attached to the same presynaptic cell, and the input signal $e_j(t) = s(t) + \xi_j(t)$ into the synapse j is taken as the superposition of a deterministic aperiodic waveform $s(t)$ and noise $\xi_j(t)$. The $\xi_j(t)$ are modeled as independent non-negative white noise sources with the same probability density function $f_\xi(u)$ for which various standard forms can be considered [57]. Here, we mainly consider the gamma probability density of order $a \geq 1$, as

$$f_\xi(u) = \begin{cases} \dfrac{1}{b^a \Gamma(a)} u^{a-1} \exp\left(-\dfrac{u}{b}\right), & u \geq 0, \\ 0, & u < 0, \end{cases} \tag{2}$$

where $\Gamma(a) = \int_0^\infty x^{a-1}\exp(-x)\mathrm{d}x$, the mean value of $\xi_j(t)$ being ab, its variance ab^2, and its rms amplitude $\xi_{\mathrm{rms}} = b\sqrt{a^2 + a}$. It is noted that the non-negative uniform noise and gamma noise were considered for improving the synaptic signal transduction, and the similar stochastic resonant behaviors for both kinds of noise have been observed in a single excitatory synapse [57].

For multiple synapses, the total synaptic current collecting several synaptic currents $I_j(t)$ as

$$I(t) = \sum_j I_j(t), \tag{3}$$

is taken as the relevant output of this multisynaptic pathway. The total synaptic current $I(t)$ forms the somatic current, which directly drives the dynamics of the membrane potential of the postsynaptic neuron. When this potential reaches the firing threshold, a spike is emitted by the neuron and its potential is reset to its resting value. This stage constitutes the well-known threshold dynamics of the neuron, which has been shown to lend itself to various forms of stochastic resonance [2–4,6,18,23–25,28,29,31,33,34,26,27]. Yet here we are not considering this threshold nonlinear dynamics of the neuron. Instead, we investigate the nonlinear saturating dynamics of Eq. (1), which takes place in synaptic transduction. Then, in order to investigate the possibilities of noise-aided signal transmission in such multisynaptic pathways, a useful input–output measure of similarity, frequently used in stochastic resonance studies, is the correlation coefficient [23,26,27,52,61,62] of

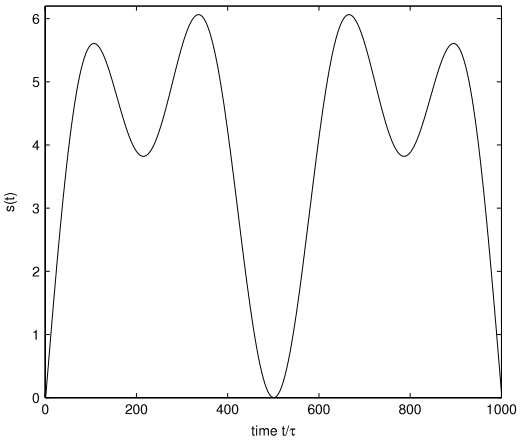

Fig. 1. An example of the input signal $s(t)$ from Eq. (5) with $T_s = 10^3\tau$, $A_1 = 5I_{\mathrm{sat},j}$, $A_2 = 3I_{\mathrm{sat},j}$ and $A_3 = 2I_{\mathrm{sat},j}$. Here, the relaxation time of saturating dynamic $\tau = 0.1$s and the saturation current $I_{\mathrm{sat},j} = 1$ in Eq. (1).

the input $s(t)$ with the output $I(t)$

$$\rho_{sI} = \frac{\overline{[s(t) - \overline{s(t)}][I(t) - \overline{I(t)}]}}{\left\{\overline{[s(t) - \overline{s(t)}]^2}\,\overline{[I(t) - \overline{I(t)}]^2}\right\}^{1/2}}, \tag{4}$$

where the overbar denotes a temporal average.

3. Simulation results

Based on the neural interpretation of Eq. (1), the input $e_j(t)$ into the synapse j is non-negative, and taken as the superposition $e_j(t) = s(t) + \xi_j(t)$ of a deterministic aperiodic waveform $s(t)$ and noise $\xi_j(t)$. Both components $s(t)$ and $\xi_j(t)$ are separately formed with the same neural substrate as $e_j(t)$, and share the same nature of non-negative quantities that describe presynaptic activity, be it a spontaneous random activity for $\xi_j(t)$ or a coherent activity for $s(t)$ [57]. The non-negative noise $\xi_j(t)$ is given in Eq. (2), and the deterministic aperiodic waveform $s(t)$ is here defined over $t \in [0, T_s]$ as

$$s(t) = A_1 \sin(\pi t/T_s) + A_2 \sin(3\pi t/T_s) + A_3 \sin(7\pi t/T_s), \tag{5}$$

with $s(t)$ being zero outside $[0, T_s]$. An example of the waveform $s(t)$ of Eq. (5) is depicted in Fig. 1. The purpose of Eq. (5) is to have a non-negative signal $s(t)$, which carries some distinctive features in the upper part of the waveform that can suffer from saturation in transmission by Eq. (1).

When the noise $\xi_j(t)$ is absent, the solution to Eq. (1) with initial condition $I_j(t_0)$ reads

$$I_j(t) = \left\{ I_j(t_0) + I_{\mathrm{sat},j} \int_{t_0}^{t} w_j\, s(t'') \exp\left[\frac{t'' - t_0}{\tau} + \int_{t_0}^{t''} w_j\, s(t')\mathrm{d}t' \right] \mathrm{d}t'' \right\} \times \exp\left[-\frac{t - t_0}{\tau} - \int_{t_0}^{t} w_j\, s(t')\mathrm{d}t' \right], \tag{6}$$

for $t \geq t_0$. Thus, in the presence of input signal $s(t)$ only, the correlation coefficient ρ_{sI} between the somatic current $I(t) = \sum_j I_j(t)$ and the input signal $s(t)$ can then be computed directly according to Eqs. (4) and (6). When the noise $\xi_j(t)$ is present at the input, the somatic current $I(t)$ will be simulated numerically [57,69], and an ensemble-averaging of the correlation coefficient ρ_{sI} will be performed over independent realizations of the noise to yield $\langle \rho_{sI} \rangle$, following the common practice in stochastic resonance studies [23,27]. In numerical simulations of Eq. (1), the Euler–Maruyama method is used [69], with a sampling time step Δt much less than the time constant τ and the signal duration T_s, and which is fixed at $\Delta t = 0.1\tau$ throughout.

3.1. Two synaptic pathways of an excitatory and an inhibitory

For a single excitatory synapse, the constructive influence of the rms noise amplitude of $\xi_1(t)$ on the synaptic current $I(t) = I_1(t)$ has been demonstrated with the appearance of the stochastic resonance effect [57], which is also numerically shown in Fig. 2(a) denoted by asterisks ($*$). Here, the excitatory synapse $j = 1$ is always subjected to the noisy input $e_1(t) = s(t) + \xi_1(t)$, and the efficacy parameter of the synapse $w_1 = 100$. The input signal $s(t)$ is with $T_s = 10^3\tau$, $A_1 = 5I_{\mathrm{sat},1}$, $A_2 = 3I_{\mathrm{sat},1}$ and $A_3 = 2I_{\mathrm{sat},1}$. It is clearly visible in Fig. 2(a) that, as the rms noise amplitude ξ_{rms} increases, the input–output ensemble-averaging of correlation coefficient $\langle \rho_{sI} \rangle$ presents a stochastic resonant behavior. In other words,

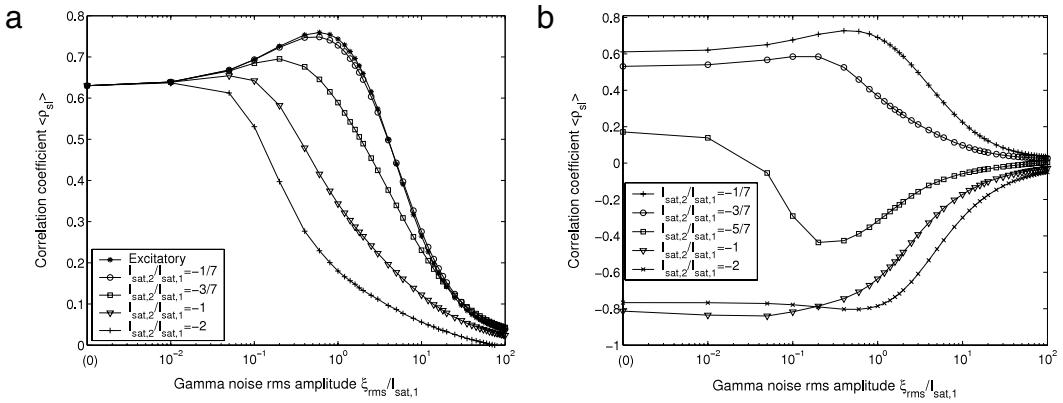

Fig. 2. Ensemble-averaged correlation coefficient $\langle\rho_{sI}\rangle$ between the input stimulus $s(t)$ and the somatic current $I(t)$, as a function of the noise rms amplitude $\xi_{\rm rms}$, for different values of the inhibitory saturation current $I_{\rm sat,2}/I_{\rm sat,1}$ indicated by the legend. The excitatory presynaptic activity is $e_1(t) = s(t) + \xi_1(t)$ and the efficacy parameter of the synapse $w_1 = 100$. The inhibitory presynaptic activity is (a) $e_2(t) = \xi_2(t)$, and (b) $e_2(t) = s(t) + \xi_2(t)$. Here, the input signal $s(t)$ from Eq. (5) is with $T_s = 10^3\tau$, $A_1 = 5I_{\rm sat,1}$, $A_2 = 3I_{\rm sat,1}$ and $A_3 = 2I_{\rm sat,1}$. The efficacy parameter of the synapse $w_2 = 50$. Here, $\xi_1(t)$ and $\xi_2(t)$ are independent gamma noise sources of order $a = 2$ with the same noise rms amplitude $\xi_{\rm rms}$. Each point was averaged over 1000 trials. For simplicity, we represent the origin tick 10^{-3} of the logarithmic x-axis as zero, and $\xi_{\rm rms}$ actually increases from zero.

an optimal amount of noise corresponds to the maximum value of $\langle\rho_{sI}\rangle$, while too little or too much noise reduces the correlation coefficient $\langle\rho_{sI}\rangle$. For the efficacy parameter of the synapse $w_1 = 100$, the system of Eq. (1) leads to the operation in the saturation region. It is seen in Fig. 2(a) that, at the level of noise $\xi_{\rm rms} = 0$, the initial correlation coefficient $\langle\rho_{sI}\rangle = 0.6301$ calculated by Eq. (6) is rather lower than unity. This indicates that, due to the saturation dynamics of Eq. (1), the distortion undergone by the input $s(t)$ results in a corresponding distorted waveform of $I(t)$ as compared with $s(t)$. However, as the noise level $\xi_{\rm rms}$ is raised above zero, Fig. 2(a) shows that the addition of noise is able to overcome this distortion imposed on $I(t)$, and a suitable amount of added noise can pull the output $I(t)$ away from the strong saturation regime, eliciting the possibility of an improvement of $\langle\rho_{sI}\rangle$ by noise in one excitatory synapse [57].

Next, we connect an inhibitory synapse $j = 2$ to the excitatory synapse $j = 1$, and the somatic current $I(t)$ is the sum of the synapse currents of $I_1(t)$ and $I_2(t)$ of two synapses $j = 1, 2$. Since a certain degree of heterogeneity both in their internal parameters and in their connectivity pattern is more popular in real populations [61], we take different values of the efficacy parameter. Here, the inhibitory synapse $j = 2$ is with the efficacy of synapse $w_2 = 50$. We observe that:

(i) When the random activity of an inhibitory synapse is $e_2(t) = \xi_2(t)$, Fig. 2(a) shows the correlation coefficient $\langle\rho_{sI}\rangle$ between the input $s(t)$ contained in the excitatory activity $e_1(t)$ and the output $I(t)$ as a function of the rms noise amplitude $\xi_{\rm rms}$, for different values of the saturation current $I_{\rm sat,2}/I_{\rm sat,1} = -1/7, \ -3/7, \ -1$ and -2. Here, $\xi_1(t)$ and $\xi_2(t)$ are independent, but with the same rms amplitude $\xi_{\rm rms}$. Since the presynaptic input $e_2(t)$ of the inhibitory synapse $j = 2$ does not contain the signal $s(t)$, $\langle\rho_{sI}\rangle$ still starts from the same value of 0.6301 at $\xi_{\rm rms} = 0$ by the excitatory dynamics of Eq. (6) driven by $e_1(t) = s(t)$. It is seen that the addition of the random activity of noise $e_2(t) = \xi_2(t)$ degrades the emergence of stochastic resonance in the single excitatory synapse $j = 1$. When the saturation current $I_{\rm sat,2}/I_{\rm sat,1}$ decreases to -2, the stochastic resonance effect disappears: a monotonic decay of $\langle\rho_{sI}\rangle$ toward zero is observed when the rms noise amplitude $\xi_{\rm rms}$ increases.

(ii) When the presynaptic activity of the inhibitory synapse $j = 2$ is $e_2(t) = s(t) + \xi_2(t)$, the correlation coefficient $\langle\rho_{sI}\rangle$ between the input signal $s(t)$ and the somatic current $I(t)$ is illustrated in Fig. 2(b) as a function of the rms noise amplitude $\xi_{\rm rms}$. It is observed in Fig. 2(b) that, as the rms noise amplitude $\xi_{\rm rms}$ takes the level of zero, the initial $\langle\rho_{sI}\rangle$ takes different initial values. The reason is that the inhibitory presynaptic activity $e_2(t)$ also receives the input signal $s(t)$, and initial $\langle\rho_{sI}\rangle$ should be calculated by summing the excitatory and inhibitory dynamics of Eq. (6) driven by $e_1(t) = e_2(t) = s(t)$. For the positive saturation current $I_{\rm sat,1}$, the output $I_1(t)$ is predicatively positive, and partly similar to the input $s(t)$. Contrarily, the output $I_2(t)$ is negative and partly similar to $-s(t)$, as the saturation current $I_{\rm sat,2}$ is always negative for the inhibitory synapse. Naturally, at the rms noise amplitude $\xi_{\rm rms} = 0$, the somatic current $I(t) = I_1(t) + I_2(t)$ is usually less similar to the input $s(t)$, and the initial $\langle\rho_{sI}\rangle$ between $I(t)$ and $s(t)$, as shown in Fig. 2(b), is less than the value of 0.6301 illustrated in Fig. 2(a) that depicts the similarity of $I_1(t)$ to $s(t)$. It is also interesting to note that, as the inhibitory saturation current $I_{\rm sat,2}/I_{\rm sat,1}$ decreases from $-1/7$ to -2, $\langle\rho_{sI}\rangle$ exhibits two opposite kinds of stochastic resonance phenomena versus the rms noise amplitude $\xi_{\rm rms}$. Here, the smaller the negative value of $\langle\rho_{sI}\rangle$ is, the closer the relationship between $I(t)$ and $-s(t)$. These resonant curves of $\langle\rho_{sI}\rangle$ plotted in Fig. 2(b) demonstrate the constructive roles of $\xi_1(t)$ and $\xi_2(t)$ for the efficacy of signal transmission through the dynamical saturating synapses in a complex way. Furthermore, as the rms noise amplitude $\xi_{\rm rms}$ increases to a very large levels, e.g. $\xi_{\rm rms}/I_{\rm sat,1} = 10^2$, as shown in Fig. 2(b), the correlation coefficients $\langle\rho_{sI}\rangle$ that correspond to a different saturation current $I_{\rm sat,2}$ congregate around the region being close to zero. This means that too much noise disturbs the somatic current $I(t)$, reducing the effect on the input signal $s(t)$ or $-s(t)$.

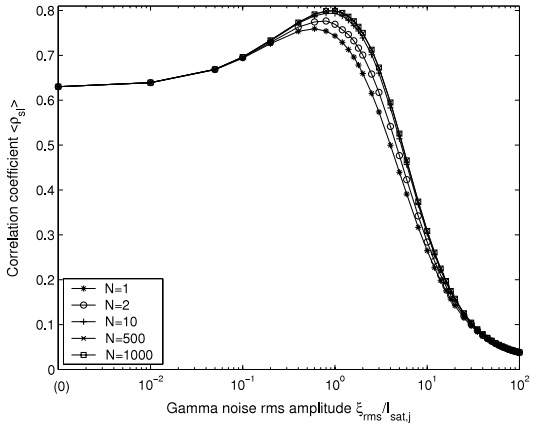

Fig. 3. Ensemble-averaged correlation coefficient $\langle \rho_{sl} \rangle$ between input $s(t)$ and output $I(t) = \sum_{j=1}^{N} I_j(t)$, as a function of the noise rms amplitude $\xi_{\rm rms}$, for different numbers of excitatory synapses $N = 1, 2, 10, 500$ and 1000 indicated by the legend. Each excitatory synapse j is with the presynaptic activity $e_j(t) = s(t) + \xi_j(t)$ and the efficacy parameter of the synapse $w_j = 100$. No inhibitory synapse is connected. For simplicity, we represent the origin tick 10^{-3} of the logarithmic x-axis as zero, and $\xi_{\rm rms}$ actually increases from zero. Other parameters are the same as in Fig. 2.

3.2. Parallel arrays of excitatory synapses and inhibitory synapses

Next, we investigate the improvement of signal transduction through a population of synapses via the constructive role of internal noise in each synapse. In particular, the study of signal transmission in parallel arrays of nonlinear systems has received considerable attention, and in such arrays, an important specific form of stochastic resonance, i.e. suprathreshold stochastic resonance, has been reported [7]. Moreover, the essential role of neuronal noise is subsequently investigated for information transmission in the context of suprathreshold stochastic resonance [37,38]. Here, we also consider a population of synapses on the same postsynaptic neuron that realizes a real-world example of the basic structure of suprathreshold stochastic resonance, aiming to observe a more remarkable improvement in a parallel bundle of synapses [26,27,39,60–63].

We first consider a parallel array of multiple synapses consisting of excitatory synapses for $j = 1, 2, \ldots, N$ with the same saturation current $I_{{\rm sat},j}$, and each is driven by $e_j(t) = s(t) + \xi_j(t)$. No inhibitory synapses are connected. Then, the collective current of synaptic pathways is $I(t) = \sum_{j=1}^{N} I_j(t)$. Fig. 3 shows the correlation coefficient $\langle \rho_{sl} \rangle$ as a function of the rms noise amplitude $\xi_{\rm rms}$, for different numbers of excitatory synapses $N = 1, 2, 10, 500$ and 1000. As the rms noise amplitude $\xi_{\rm rms}$ increases from zero, the feature of stochastic resonance is obviously demonstrated by the bell-type curve of $\langle \rho_{sl} \rangle$ versus $\xi_{\rm rms}$. It is seen in Fig. 3 that, as the number of excitatory synapses N increases, the ensemble collective property of noise $\xi_j(t)$ in each excitatory synapses $j = 1, 2, \ldots, N$ can further enhance the correlation coefficient $\langle \rho_{sl} \rangle$. For instance, the maximum of $\langle \rho_{sl} \rangle$ can be improved to 0.8001 at $\xi_{\rm rms}/I_{{\rm sat},j} = 1.12$ for a parallel array of $N = 1000$ excitatory synaptic pathways. In view of the input signal $s(t)$ being with $A_1 = 5I_{{\rm sat},j}$, $A_2 = 3I_{{\rm sat},j}$ and $A_3 = 2I_{{\rm sat},j}$, this enhancement effect of $\langle \rho_{sl} \rangle$ by both the noise $\xi_j(t)$ and the parallel array size N can be regarded as a specific form of suprathreshold stochastic resonance [7] in a broad sense. The obtained results of Fig. 3 also indicate the strategy of assembling excitatory synaptic pathways into an uncoupled parallel array to improve signal transduction at the synaptic stage is possible and advantageous.

We further explore the signal transduction in a parallel array of multiple synapses composed of both excitatory synapses $j = 1, 2, \ldots, N$, with the same saturation current $I_{{\rm sat},j}$, and inhibitory synapses $k = 1, 2, \ldots, M$, with the same saturation current $I_{{\rm sat},k}$. Then, the somatic current becomes $I(t) = \sum_{j=1}^{N} I_j(t) + \sum_{k=1}^{M} I_k(t)$. Correspondingly, $\xi_j(t)$ and $\xi_k(t)$ are also mutually independent, but with a same rms noise amplitude $\xi_{\rm rms}$. Here, the excitatory synapses are always subjected to the noisy input stimuli $e_j(t) = s(t) + \xi_j(t)$, while two kinds of the inhibitory synaptic input $e_k(t)$ are considered:

(i) First, each inhibitory synapse k is driven by the random activity of $e_k(t) = \xi_k(t)$ for $k = 1, 2, \ldots, M$. The corresponding correlation coefficient $\langle \rho_{sl} \rangle$ versus the noise amplitude $\xi_{\rm rms}$ is shown in Fig. 4. In Fig. 4(a), the saturation current $I_{{\rm sat},k}/I_{{\rm sat},j} = -5/7$ is fixed, while the numbers of synapses $N = M$ increase from unity to 1000. It is seen in Fig. 4(a) that the array stochastic resonance effect is clearly visible: The larger the number of the parallel arrays of synaptic pathways is, the more prominent the correlation coefficient $\langle \rho_{sl} \rangle$ is enhanced by the noise sources $\xi_j(t)$ and $\xi_k(t)$. It is seen that when the numbers of the multiple synaptic pathways increase as $N = M \geq 500$, the curves of $\langle \rho_{sl} \rangle$ converge. For the multiple synaptic pathways with large synaptic numbers $N = M = 1000$ (down triangles), the maximum of $\langle \rho_{sl} \rangle$ can be enhanced to 0.886 at $\xi_{\rm rms}/I_{{\rm sat},j} = 2.5$. Compared with Fig. 3, obtained by only the multiple excitatory synaptic pathways, this improvement of $\langle \rho_{sl} \rangle$ of 0.886 is quite evident. Furthermore, we plot the correlation coefficient $\langle \rho_{sl} \rangle$ versus the rms noise amplitude $\xi_{\rm rms}$ in Fig. 4(b) for different inhibitory saturation currents $I_{{\rm sat},k}/I_{{\rm sat},j}$ and the same numbers of synapses $N = M = 1000$. It is shown in Fig. 4(b) that, for the inhibitory saturation current $I_{{\rm sat},k}/I_{{\rm sat},j} = -1$ (squares), the maximum of $\langle \rho_{sl} \rangle$ can be further improved to 0.9241 at $\xi_{\rm rms}/I_{{\rm sat},1} = 9.7$, whereby the collective effect of synaptic noise sources $\xi_j(t)$ and $\xi_k(t)$ on the correlation coefficient $\langle \rho_{sl} \rangle$ is optimized. It is observed in Fig. 4(b) that other values of $I_{{\rm sat},2}/I_{{\rm sat},1}$ cannot acquire this optimal value of the correlation coefficient $\langle \rho_{sl} \rangle$. Finally, the inhibitory saturating current $I_{{\rm sat},k}/I_{{\rm sat},j} = -1$ and

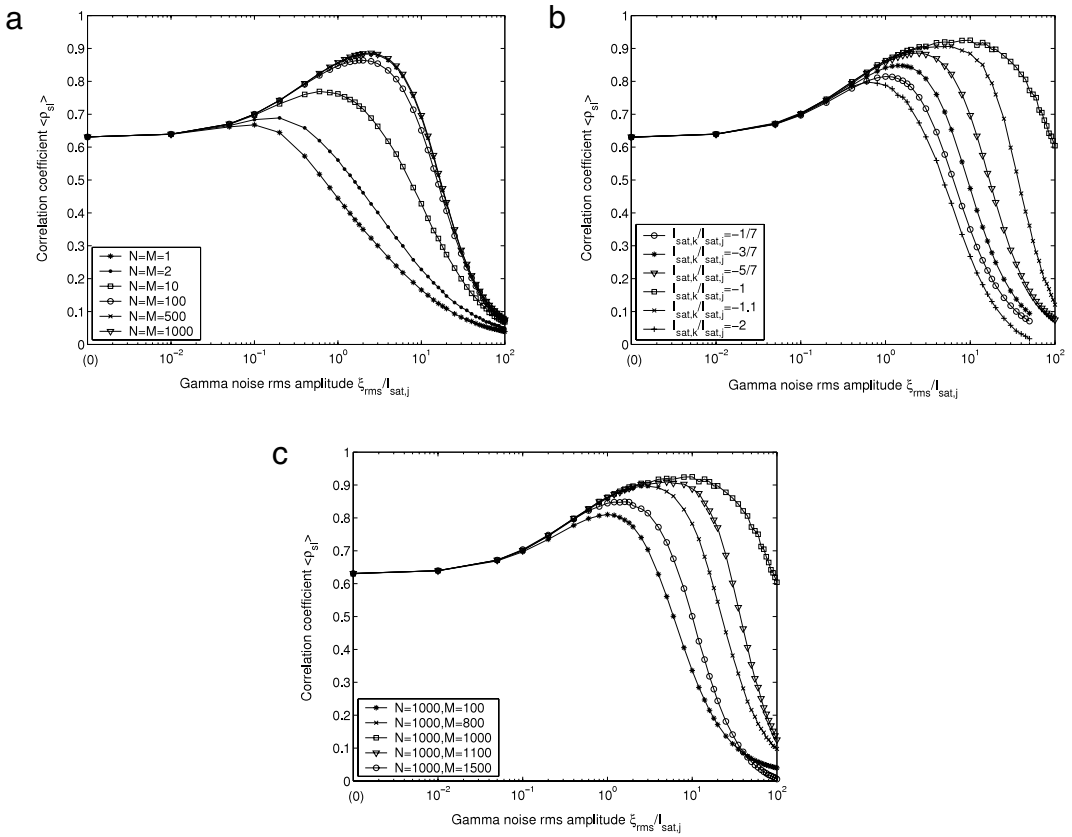

Fig. 4. Ensemble-averaged correlation coefficient $\langle \rho_{sI} \rangle$ between input $s(t)$ and the somatic current $I(t) = \sum_{j=1}^{N} I_j(t) + \sum_{k=1}^{M} I_k(t)$, as a function of the noise rms amplitude $\xi_{\rm rms}$. Here, the inhibitory pathway is combined in parallel with the excitatory pathway, resulting in parallel arrays of multiple synapses. Note that each inhibitory synapse k is purely driven by the random activity of $e_k(t) = \xi_k(t)$ for $k = 1, 2, \ldots, M$, while each excitatory synapse j is with the presynaptic activity $e_j(t) = s(t) + \xi_j(t)$. The efficacy parameters of the synapse are $w_j = 100$ and $w_k = 50$, respectively. (a) The numbers of synapses are $N = M = 1$, 2, 10, 100, 500 and 1000, while the saturation current $I_{{\rm sat},k}/I_{{\rm sat},j} = -5/7$ is fixed; (b) The inhibitory saturation currents $I_{{\rm sat},k}/I_{{\rm sat},j} = -1/7, -3/7, -5/7, -1, -1.1$ and -2, but the numbers of synapses $N = M = 1000$ are fixed; (c) The inhibitory saturation current $I_{{\rm sat},k}/I_{{\rm sat},j} = -1$ and the number of excitatory synapses $N = 1000$ are fixed, while the number of inhibitory synapses M varies. For simplicity, we represent the origin tick 10^{-3} of the logarithmic x-axis as zero, and $\xi_{\rm rms}$ actually increases from zero. Other parameters are the same as in Fig. 2.

the number of excitatory synapses $N = 1000$ are fixed, while the parallel inhibitory synapses vary their connected number M. The obtained results of $\langle \rho_{sI} \rangle$ versus $\xi_{\rm rms}$ are then shown in Fig. 4(c), which indicates the number of $M = 1000$ (squares) corresponds to the best behavior of $\langle \rho_{sI} \rangle$ as $\xi_{\rm rms}$ increases.

In this case of the parallel inhibitory synapses $k = 1, 2, \ldots, M$ driven by pure random activities $e_k(t) = \xi_k(t)$, the synaptic currents $I_k(t)$ are all negative. When these negative currents $I_k(t)$ are added to the outputs $I_j(t)$ of excitatory synapses $j = 1, 2, \ldots, N$, the summed result of somatic current $I(t)$ manifests more similar to the input $s(t)$. This collective property of $\xi_k(t)$ in inhibitory synapses seems to counteract the influence of $\xi_j(t)$ in excitatory synapses on the output $I(t)$, leading to a great improvement of $\langle \rho_{sI} \rangle$ shown in Fig. 4.

(ii) Next, we assume the inhibitory presynaptic activity as $e_k(t) = s(t) + \xi_k(t)$ for $k = 1, 2, \ldots, M$. Two representative examples of the corresponding correlation coefficient $\langle \rho_{sI} \rangle$ are illustrated in Fig. 5(a) and (b). In Fig. 5(a), the inhibitory saturation currents $I_{{\rm sat},k}/I_{{\rm sat},j} = -1/7$, and the behaviors of $\langle \rho_{sI} \rangle$ versus the noise amplitude $\xi_{\rm rms}$ are plotted for different synaptic numbers $N = M = 1$, 2, 10, 100 and 1000. Since $|I_{{\rm sat},k}|$ is relatively smaller than $I_{{\rm sat},j}$, the initial correlation coefficient $\langle \rho_{sI} \rangle$ is still positive according to Eq. (6). As the rms noise amplitude $\xi_{\rm rms}$ increases, $\langle \rho_{sI} \rangle$ is first raised to the maximum value, and then degrades gradually, which are the typical convex curves of stochastic resonance. Conversely, for the inhibitory saturating currents $I_{{\rm sat},k}/I_{{\rm sat},j} = -1$, the initial correlation coefficient $\langle \rho_{sI} \rangle$ is negative. Note that $\langle \rho_{sI} \rangle$ is improved towards -1 in absolute value as the rms noise amplitude $\xi_{\rm rms}$ increases. As we explained, the negative value of $\langle \rho_{sI} \rangle$ in Fig. 2(b) denotes that the somatic current of $I(t)$ is similar to the input $-s(t)$. The constructive role of noise and the collective effect of synaptic numbers N and M on $\langle \rho_{sI} \rangle$ can be also regarded as a kind of stochastic resonance effect. However, in order to obtain the positive values of $\langle \rho_{sI} \rangle$, the case of entering only random activity $e_k(t) = \xi_k(t)$ into the inhibitory synapses, as shown in Fig. 3, is preferable to this case of the inhibitory synapses with the presynaptic activity taking $e_k(t) = s(t) + \xi_k(t)$ of Fig. 5.

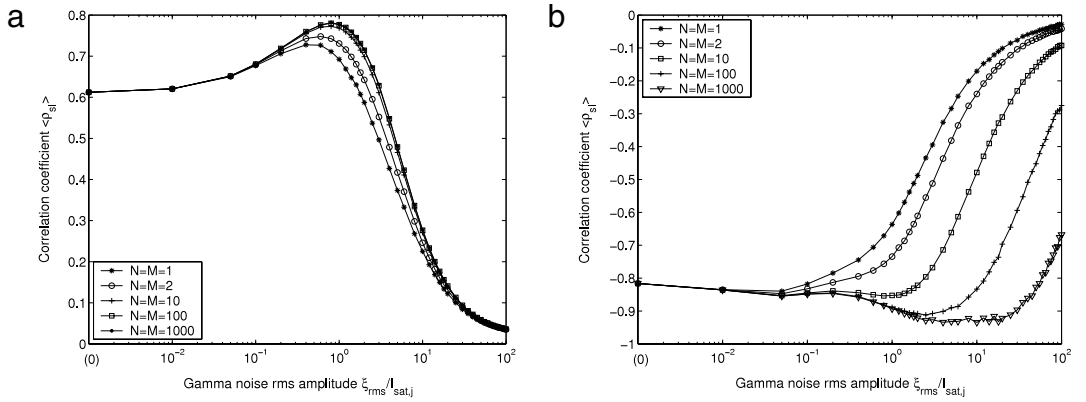

Fig. 5. Ensemble-averaged correlation coefficient $\langle \rho_{sI} \rangle$ between input $s(t)$ and output $I(t)$, as a function of the noise rms amplitude $\xi_{\rm rms}$. Here, each inhibitory synapse k is driven by $e_k(t) = s(t) + \xi_k(t)$ for $k = 1, 2, \ldots, M$, and each excitatory synapse j is with the presynaptic activity $e_j(t) = s(t) + \xi_j(t)$. The efficacy parameter of the synapse $w_j = 100$ and $w_k = 50$, respectively. The numbers of synapses $N = M = 1, 2, 10, 100, 500$ and 1000, while the saturation current (a) $I_{{\rm sat},k}/I_{{\rm sat},j} = -1/7$ and (b) $I_{{\rm sat},k}/I_{{\rm sat},j} = -1$. For simplicity, we represent the origin tick 10^{-3} of the logarithmic x-axis as zero, and $\xi_{\rm rms}$ actually increases from zero. Other parameters are the same as in Fig. 2.

4. Conclusion

In this paper, we studied the signal transmission in parallel arrays of synapses composed of both the excitatory synaptic pathway and the inhibitory synaptic pathway at the synaptic stage. The corresponding synaptic currents from the excitatory synaptic pathways and the inhibitory synaptic pathways are summed as the somatic current of multiple synaptic pathways. For a single excitatory synapse, the combination of an inhibitory synapse does not enhance the stochastic resonance effect. When large numbers of excitatory synapses are assembled as a parallel array, as compared with a single excitatory synapse, the improvement of the correlation coefficient by noise can be slightly increased. Interestingly, the enhancement of correlation coefficient by noise can be greatly improved by introducing inhibitory pathways into the parallel arrays of multiple synaptic pathways, and the independent noise sources in multiple synaptic pathways play an integrated constructive role on signal transduction by increasing the synaptic numbers as well as the rms noise amplitude. We argue that the negative output of inhibitory synapses purely driven by random noise can mostly counteract the influence of synaptic noise in excitatory pathways on the somatic current, resulting in the prominent improvement of the input–output correlation coefficient illustrated in Fig. 4. Since processing of neural information usually involves integration of excitatory and inhibitory synaptic inputs [64,60,61], the observation of stochastic resonance in the noisy multiple synaptic pathways considered in this paper points to a useful mechanism accessible to neural signals at the synaptic stage. The possibility of stochastic resonance for neural signal transduction motivates the need for further experiments on live neurons.

Acknowledgments

This work is sponsored by the Taishan Scholar CPSP and the Natural Science Foundation of Shandong Province, China (No. ZR2010FM006). Funding from the Australian Research Council (ARC) is gratefully acknowledged.

References

[1] R. Benzi, A. Sutera, A. Vulpiani, The mechanism of stochastic resonance, Journal of Physics A: Mathematical and General 14 (1981) L453–L457.
[2] L. Gammaitoni, P. Hänggi, P. Jung, F. Marchesoni, Stochastic resonance, Reviews of Modern Physics 70 (1998) 233–287.
[3] A. Longtin, Stochastic resonance in neuron models, Journal of Statistical Physics 70 (1993) 309–327.
[4] K. Wiesenfeld, F. Moss, Stochastic resonance and the benefits of noise: from ice ages to crayfish and squids, Nature 373 (1995) 33–36.
[5] J.J. Collins, C.C. Chow, A.C. Capela, T.T. Imhoff, Aperiodic stochastic resonance, Physical Review E 54 (1996) 5575–5584.
[6] M.D. Mc Donnell, D. Abbott, What is stochastic resonance? definitions, misconceptions, debates, and its relevance to biology, PLoS Computational Biology 5 (2009) art. no. e1000348.
[7] N.G. Stocks, Suprathreshold stochastic resonance in multilevel threshold systems, Physical Review Letters 84 (2000) 2310–2313.
[8] L. Torok, L.B. Kish, Integro–differential stochastic resonance, Fluctuation and Noise Letters 5 (2005) L27–L42.
[9] J. Li, B. Xu, Binary information processing via parameter-induced stochastic resonance in the presence of multiplicative and additive colored noise with colored cross-correlation, International Journal of Bifurcation and Chaos 16 (2006) 427–435.
[10] J. Li, B. Xu, Effects of signal spectrums on signal processing by parameter-induced stochastic resonance, Physica A: Statistical Mechanics and its Applications 361 (2006) 11–23.
[11] D. Rousseau, J. Rojas Varela, F. Chapeau-Blondeau, Stochastic resonance for nonlinear sensors with saturation, Physical Review E 67 (2003) art. no. 021102.
[12] D. Rousseau, F. Chapeau-Blondeau, Neuronal signal transduction aided by noise at threshold and at saturation, Neural Processing Letters 20 (2004) 71–83.
[13] F. Chapeau-Blondeau, S. Blanchard, D. Rousseau, Noise-enhanced fisher information in parallel arrays of sensors with saturation, Physical Review E 74 (2006) art. no. 031102.
[14] F. Chapeau-Blondeau, D. Rousseau, Noise-aided SNR amplification by parallel arrays of sensors with saturation, Physics Letters A 351 (2006) 231–237.

[15] S. Blanchard, D. Rousseau, F. Chapeau-Blondeau, Noise enhancement of signal transduction by parallel arrays of nonlinear neurons with threshold and saturation, Neurocomputing 71 (2007) 333–341.
[16] M. Ueda, Improvement of signal-to-noise ratio by stochastic resonance in sigmoid function threshold systems demonstrated using a CMOS inverter, Physica A: Statistical Mechanics and its Applications 389 (2010) 1978–1985.
[17] F. Duan, F. Chapeau-Blondeau, D. Abbott, Input–output gain of collective response in an uncoupled parallel array of saturating dynamical subsystems, Physica A: Statistical Mechanics and its Applications 388 (2009) 1345–1351.
[18] F. Duan, F. Chapeau-Blondeau, D. Abbott, Enhancing array stochasatic resonance in ensembles of excitable systems, Journal of Statistical Mechanics: Theory and Experiment 8 (2009) art. no. P08017.
[19] M.I. Dykman, D.G. Luchinsky, R. Mannella, P.V.E. McClintock, H.E. Short, N.D. Stein, N.G. Stocks, Noise-induced linearization, Physics Letters A 193 (1994) 61–66.
[20] N.G. Stocks, N.D. Stein, H.E. Short, R. Mannella, D.G. Luchinsky, P.V.E. Mc Clintock, M.I. Dykman, Noise-induced linearization and delinearization, in: M. Millonas (Ed.), Fluctuations and Order: The New Synthesis, Springer, Berlin, 1993, pp. 53–67.
[21] L. Gammaitoni, Stochastic resonance and the dithering effect in threshold physical systems, Physical Review E 52 (1995) 4691–4698.
[22] R.A. Wannamaker, S.P. Lipshitz, J. Vanderkooy, Stochastic resonance as dithering, Physical Review E 61 (2000) 233–236.
[23] J.J. Collins, C.C. Chow, T.T. Imhoff, Stochastic resonance in neuron models, Physical Review E 52 (1995) R3321–R3324.
[24] A. Bulsara, E. Jacobs, T. Zhou, F. Moss, L. Kiss, Stochastic resonance in a single neuron model: theory and analog simulation, Journal of Theoretical Biology 152 (1991) 531–555.
[25] A. Longtin, A. Bulsara, F. Moss, Time interval sequences in the bistable systems and the noise induced transmission of information by sensory neurons, Physical Review Letters 67 (1991) 656–659.
[26] B. Lindner, J. García-Ojalvo, A. Neiman, L. Schimansky-Geier, Effects of noise in excitable systems, Physics Reports 392 (2004) 321–424.
[27] J.J. Collins, C.C. Chow, T.T. Imhoff, Stochastic resonance without tuning, Nature 376 (1995) 236–238.
[28] A.R. Bulsara, T.C. Elton, C.R. Doering, S.B. Lowen, K. Lindenberg, Cooperative behavior in periodically driven noisy intergate-fire models of neuronal dynamics, Physical Review E 53 (1996) 3958–3969.
[29] F. Chapeau-Blondeau, X. Godivier, N. Chambet, Stochastic resonance in a neuron model that transmits spike trains, Physical Review E 53 (1996) 1273–1275.
[30] X. Godivier, F. Chapeau-Blondeau, Noise-enhanced transmission of spike trains in the neuron, Europhysics Letters 35 (1996) 473–477.
[31] M. Stemmler, A single spike suffices: the simplest form of stochastic resonance in model neurons, Network: Computation In Neural Systems 7 (1996) 687–716.
[32] J.R.R. Duarte, M.V.D. Vermelho, M.L. Lyra, Stochastic resonance of a periodically driven neuron under non-Gaussian noise, Physica A: Statistical Mechanics and its Applications 387 (2008) 1446–1454.
[33] B. Kosko, S. Mitaim, Robust stochastic resonance for simple threshold neurons, Physical Review E 70 (2004) art. no. 031911.
[34] A. Patel, B. Kosko, Stochastic resonance in noisy spiking retinal and sensory neuron models, Neural Networks 18 (2005) 467–478.
[35] L.B. Kish, G.P. Harmer, D. Abbott, Information transfer rate of neurons: stochastic resonance of Shannon's information channel capacity, Fluctuation and Noise Letters 1 (2001) L13–L19.
[36] Y. Gong, Y. Xie, Y. Hao, Coherence resonance induced by non-Gaussian noise in a deterministic Hodgkin–Huxley neuron, Physica A: Statistical Mechanics and its Applications 388 (2009) 3759–3764.
[37] N.G. Stocks, R. Mannella, Generic noise-enhanced coding in neuronal arrays, Physical Review E 64 (2001) art. no. 030902(R).
[38] M.D. Mc Donnell, N.G. Stocks, C.E.M. Pearce, D. Abbott, Stochastic Resonance: From Suprathreshold Stochastic Resonance to Stochastic Signal Quantization, Cambridge University Press, 2008.
[39] F. Moss, X. Pei, Neurons in parallel, Nature 376 (1995) 211–212.
[40] W.J. Rappel, A. Karma, Noise-induced coherence in nueral network, Physical Review Letters 77 (1996) 3256–3259.
[41] D.R. Chialvo, A. Longtin, J. Mullergerking, Stochastic resonance in models of neuronal ensembles, Physical Review E 55 (1997) 1798–1808.
[42] S.K. Han, W.S. Kim, H. Kook, Temporal segmentation of the stochastic oscillator neural network, Physical Review E 58 (1998) 2325–2333.
[43] G. Mato, Stochastic resonance using noise generated by a neural network, Physical Review E 59 (1999) 3339–3343.
[44] G. Schmid, I. Goychuk, P. Hänggi, Stochastic resonance as a collective property of ion channel assemblies, Europhysics Letters 56 (2001) 22–28.
[45] Y. Sakumura, S. Ishii, Stochastic resonance with differential code in feedforward network with intra-layer random connections, Neural Networks 19 (2006) 469–476.
[46] O.Á. Åkerberg, M.J. Chacron, Noise shaping in neural population, Physical Review E 79 (2009) art. no. 011914.
[47] G. Balazsi, L.B. Kish, F. Moss, Spatiotemporal stochastic resonance and its consequences in neural model systems, Chaos 11 (2001) 563–569.
[48] J.T. Claudio, S.W. Horacio, Stochastic resonance in an extended FitzHugh–Nagumo system: the role of selective coupling, Physica A: Statistical Mechanics and its Applications 374 (2007) 46–54.
[49] J.K. Douglass, L. Wilkens, E. Pantazelou, F. Moss, Noise enhancement of information transfer in crayfish mechanoreceptors by stochastic resonance, Nature 365 (1993) 337–340.
[50] H.A. Braun, H. Wissing, K. Schäfer, M.C. Hirsch, Oscillation and noise determine signal transduction in shark multimodal sensory cells, Nature 367 (1994) 270–273.
[51] B.J. Gluckman, T.I. Netoff, E.J. Neel, W.L. Ditto, M.L. Spano, S. Schiff, Stochastic resonance in a neural network from mammalian brain, Physical Review Letters 77 (1996) 4098–4101.
[52] J.J. Collins, T.T. Imhoff, P. Grigg, Noise-enhanced information transmission in rat SA1 cutaneous mechanoreceptors via aperiodic stochastic resonance, Journal of Neurophysiology 76 (1996) 642–645.
[53] D.F. Russell, L.A. Wilkens, F. Moss, Use of behavioral stochastic resonance by paddle fish for feeding, Nature 402 (1999) 291–294.
[54] P.E. Greenwood, L.M. Ward, D.R. Russell, A. Neiman, F. Moss, Stochastic resonance enhances the electrosensory information available to paddlefish for prey capture, Physical Review Letters 84 (2000) 4773–4776.
[55] N.T. Dhruv, J.B. Niemi, J.D. Harry, L.A. Lipsitz, J.J. Collins, Enhancing tactile sensation in older adults with electrical noise stimulation, Neuroreport 13 (2002) 597–600.
[56] P. Hänggi, Stochastic resonance in biology: how noise can enhance detection of weak signals and help improve biological information processing, ChemPhysChem 3 (2002) 285–290.
[57] F. Chapeau-Blondeau, F. Duan, D. Abbott, Synaptic signal transduction aided by noise in a dynamical saturating model, Physical Review E 81 (2010) art. no. 021124.
[58] F. Chapeau-Blondeau, N. Chambet, Synapse models for neural networks: from ion channel kinetics to multiplicative coefficient w_{ij}, Neural Computation 7 (1995) 713–734.
[59] A.A. Faisal, L.P.J. Selen, D.M. Wolpert, Noise in the nervous system, Nature Reviews Neuroscience 9 (2008) 292–303.
[60] C. Koch, I. Segev, Methods in Neuronal Modeling, MIT Press, Cambridge, MA, 1989.
[61] P. Dayan, L.F. Abbott, Theoretical Neuroscience: Computational and Mathematical Modeling of Neural Systems, MIT Press, Cambridge, MA, 2001.
[62] A.V. Holden, Signal processing: neural coding by correlation? Nature 428 (2004) 328.
[63] J.M. Fellous, M. Rudolph, A. Destexhe, T.J. Sejnowski, Synaptic background noise controls the input/output characteristics of single cells in an in vitro model of in vivo activity, Neuroscience 122 (2003) 811–829.
[64] J.N. Levinson, A. El-Husseini, Building excitatory and inhibitory synapses: balancing neuroligin partnerships, Neuron 48 (2005) 171–174.
[65] M. Mattia, P.D. Giudice, Finite-size dynamics of inhibitory and excitatory interacting spiking neurons, Physical Review E 70 (2004) art. no. 052903.
[66] E.I. Volkov, M.N. Stolyarov, A.A. Zaikin, J. Kurths, Coherence resonance and polymodality in inhibitory coupled excitable oscillators, Physical Review E 67 (2003) art. no. 066202.
[67] E. Franén, A synapse which can switch from inhibitory to excitatory and back, Neurocomputing 65–66 (2005) 39–45.
[68] L. Badel, W. Gerstner, M.J.E. Richardson, Spike-triggered averages for passive and resonant neurons receiving filtered excitatory and inhibitory synaptic drive, Physical Review E 78 (2008) art. no. 011914.
[69] D.J. Higham, An algorithmic introduction to numerical simulation of stochastic differential equations, SIAM Review 43 (2001) 525–546.